DOI: 10.1002/chem.201000502

Polyelectrolyte-Assisted Formation of Molecular Nanoparticles Exhibiting Strongly Enhanced Fluorescence

Ch. G. Chandaluri,[a] A. Patra,[a, b] and T. P. Radhakrishnan*[a]

Abstract: A polyelectrolyte-assisted reprecipitation method is developed to fabricate nanoparticles of highly soluble molecules. The approach is demonstrated by using a zwitterionic diaminodicyanoquinodimethane molecule bearing remote ammonium functionalities with high solubility in water as well as organic solvents. Nanoparticles are prepared by injecting aqueous solutions of this compound containing an optimum concentration of sodium poly(styrenesulfonate) into methanol. The strong fluorescence exhibited by the compound in the aggregated state is reflected in the enhanced fluorescence of the polyelectrolyte complex in water. The nanoparticles formed in the colloidal state manifest even stronger fluorescence, which leads to an overall enhancement by about 90 times relative to aqueous solutions of the pure compound. The conditions for achieving the emission enhancement are optimized and a model for the molecular-level interactions and aggregation effects is developed through a range of spectroscopy, microscopy, and calorimetry investigations and control experiments.

Keywords: fluorescence · nanoparticles · polyelectrolytes · quinodimethanes · zwitterions

Introduction

Molecular materials, with their inherent ability to be tailored and ease of fabrication, have emerged as important candidates for the development of various electronic, photonic, and optoelectronic devices. Applications such as displays and sensors require efficient light-emitting materials. Even though a vast repertoire of highly luminescent organic molecules exists, those that can be deployed in such applications are limited due to aggregation-induced quenching effects in most of them. This has triggered extensive research aimed at identifying molecules that exhibit enhanced fluorescence in aggregate structures and in the solid state; examples of molecules developed are sterically crowded siloles,[1] poly(*p*-phenyleneethynylene)s,[2] cyanobis(biphenyl)ethenes,[3] cruciform pentamers,[4] diaminodicyanoquinodimethanes,[5,6] diphenylbutadienes,[7] and tetraphenylethenes.[8] Enhanced emission in the solid state in these materials has been attributed to a variety of effects including restricted intramolecular motion,[1,8] efficient interchain interaction and planarization,[2] and ground-state conformational change.[3] The enhanced fluorescence in the solid state exhibited by the remote functionalized diaminodicyanoquinodimethanes investigated in our laboratory has been explained in terms of the suppression of excited-state geometry relaxation.[5] The remote functionalities facilitate various intermolecular interactions as well as improve the solubility in aqueous and organic solvents. The latter aspect is of particular relevance in fabricating doped polymer thin films, which show interesting phenomena such as solvent-vapor-induced fluorescence switching.

Several of the molecules exhibiting enhanced fluorescence in the bulk solid state are also capable of strong light emission when formed as nanoparticles in the colloidal state.[4,8,9] Such luminescent nanomaterials are useful in applications such as organic light-emitting diodes, biological probes, and sensors.[10] We have investigated the size dependence of the optical[11] and nonlinear optical[12] responses of molecular nano/microcrystals of bis(haloanilino)dicyanoquinodimethanes and the strong blue fluorescence of nanocrystals of

[a] C. G. Chandaluri, Dr. A. Patra, Prof. T. P. Radhakrishnan
School of Chemistry
University of Hyderabad
Hyderabad 500046 (India)
Fax: : (+91) 40-2301-2460
E-mail: tprsc@uohyd.ernet.in

[b] Dr. A. Patra
Present address: PPSM, ENS Cachan, CNRS, UniverSud
61 Avenue du President Wilson, 94235 Cachan (France)

Supporting information for this article is available on the WWW under http://dx.doi.org/10.1002/chem.201000502. It contains details of synthesis and characterization, spectroscopy, microscopy, and calorimetry experiments.

tris(cyanophenyl)amine.[13] The most general and widely used route to the formation of molecular nanocrystals is the reprecipitation technique, wherein the solution of the compound in a suitable solvent is rapidly injected into a nonsolvent, under vigorous stirring or ultrasonication.[14] This approach is unviable in the case of molecules such as the remote functionalized diaminodicyanoquinodimethanes, which show appreciable solubility in all common solvents.[5] We have considered a solution to this problem that may have broad applicability in similar situations with other molecules; it involves the introduction of a polyelectrolyte that can bind the diaminodicyanoquinodimethanes bearing ionic groups and impart the required level of insolubility in an appropriate medium. Such an approach also raises fundamental questions related to the interaction of dye molecules or their aggregates with polymers including biological macromolecules, and its impact on the optical responses of the resulting nanostructures. Macromolecules present in the nonsolvent during reprecipitation are known to modify the size, shape, and agglomeration of microcrystals and affect their optical spectra.[15] Polyelectrolytes have been used to isolate fluorophores, for example in layer-by-layer assemblies, to circumvent self-quenching and enhance the fluorescence.[16] However, to the best of our knowledge, the utilization of polyelectrolytes to induce the reprecipitation itself and the formation of molecular nanoparticles exhibiting strongly enhanced fluorescence has not been demonstrated.

We have chosen 7,7-bis(piperazinium)-8,8-dicyanoquinodimethane bis(*p*-toluenesulfonate) ($B^{2+}[T^-]_2$ or simply BT_2) and sodium poly(styrenesulfonate) (NaPSS; Figure 1) to explore the idea described above. The synthesis and crystal structure[17] as well as enhanced fluorescence in the solid state and doped polymer films[5] of BT_2 have been reported by us earlier; the mechanism proposed for the enhanced fluorescence is shown in Figure 1. Due to the solubility of BT_2 in water and common organic solvents, attempts to prepare its nanocrystals by reprecipitation were unsuccessful. We describe a simple polyelectrolyte-assisted reprecipitation method for the fabrication of BT_2 nanoparticles in a colloidal state, and their characterization by microscopy studies. In the aqueous medium, complexation with the polyelectrolyte enhances the fluorescence of BT_2, the effect increasing with the ratio of the polymer to BT_2 and saturating at high values. Significantly, the colloids formed by injecting the aqueous solution into methanol exhibit very high fluorescence enhancement ($\approx$90 times) relative to the aqueous solution of BT_2. These observations are in sharp contrast with the report of the suppression or limited increase (in a narrow range of stoichiometries) of the fluorescence response of dyes such as rhodamine and cyanine upon interaction with poly(styrenesulfonate).[18] Several experiments are carried out to assess the conditions required to obtain maximum fluorescence enhancement of BT_2, establish the role of the polyelectrolyte, and gain a molecular-level understanding of the phenomenon. The potential impacts of the medium viscosity and ionic strength are probed. Isothermal titration calorimetry (ITC) provides information on the interactions between BT_2 and NaPSS. The current study illustrates a simple methodology to fabricate strongly fluorescent, stable aggregates of highly soluble compounds by using the reprecipitation approach.

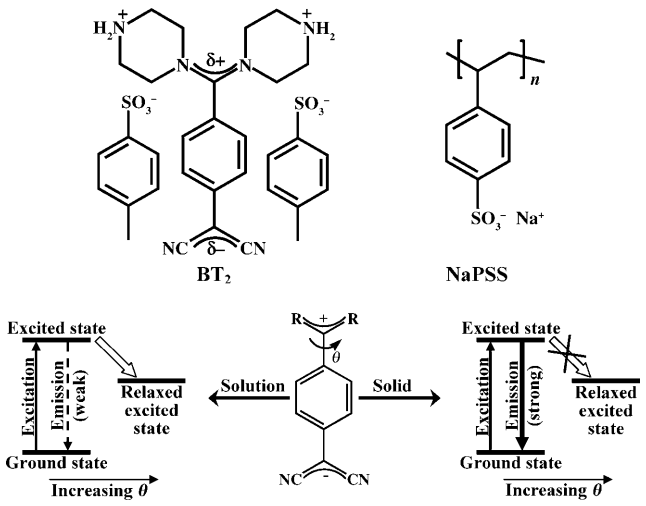

Figure 1. Molecular structure of BT_2 (the water of crystallization observed in the crystal is not shown) and NaPSS, and a schematic representation of the mechanism for fluorescence enhancement proposed in ref. [5].

Results and Discussion

Absorption and emission spectra of BT_2 in water and methanol are presented in Figure 2. The absorption with λ_{max}

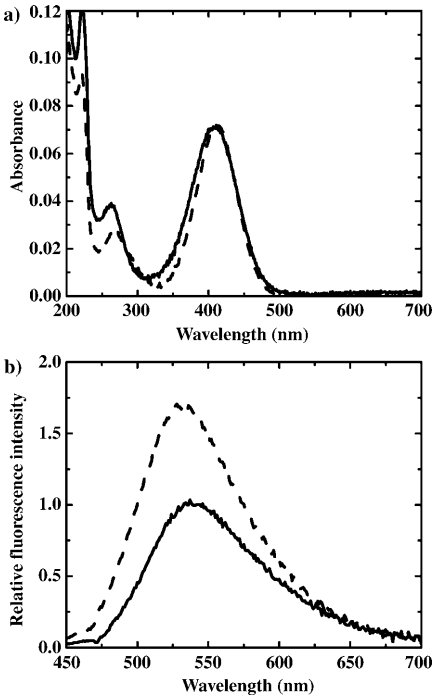

Figure 2. a) Electronic absorption and b) fluorescence emission spectra of BT_2 in water (——) and methanol (-----) solutions; λ_{exc} for the fluorescence spectra are 410 and 412 nm in water and methanol, respectively.

≈410 nm is due to the characteristic intramolecular charge transfer of the zwitterionic diaminodicyanoquinodimethanes, and the small redshift in methanol results from solvatochromic effects.[17,19] Figure 3 shows the absorption and emission spectra of aqueous solutions with a fixed concentration (6.5 μM) of BT_2 and increasing concentrations of NaPSS; the weight ratio NaPSS:BT_2, x, ranges from 20 to 500, the corresponding molar ratios being 66 to 1660 (based on the molecular weight of NaPSS monomer). The increasing optical density in the UV region is due to polyelectrolyte absorption. There is a redshift of the absorption peak of BT_2 when NaPSS is introduced, from 410 to ≈426 nm; the gradual increase of the λ_{max} and its saturation beyond a molar ratio of ≈5.0 are seen in the inset of Figure 3a. The redshift suggests that the B^{2+} units, initially solvated by pure water, move to a relatively less polarizable local environment upon binding to the polyelectrolyte chain. The molar ratio at which the shift saturates is higher than that expected based on the charge on B^{2+}, possibly due to the influence of neighboring ionic sites. More interestingly, the increasing content of NaPSS leads to an appreciable enhancement of the emission intensity. It may be noted that, as the optical density is similar in all cases (Figure 3a), the emission spectra recorded on solutions with exactly matched optical density at their absorption or excitation λ_{max} appear very similar to those in Figure 3b.[20] When $x=500$, the fluorescence intensity is about ten times higher than that of pure BT_2 in water. With

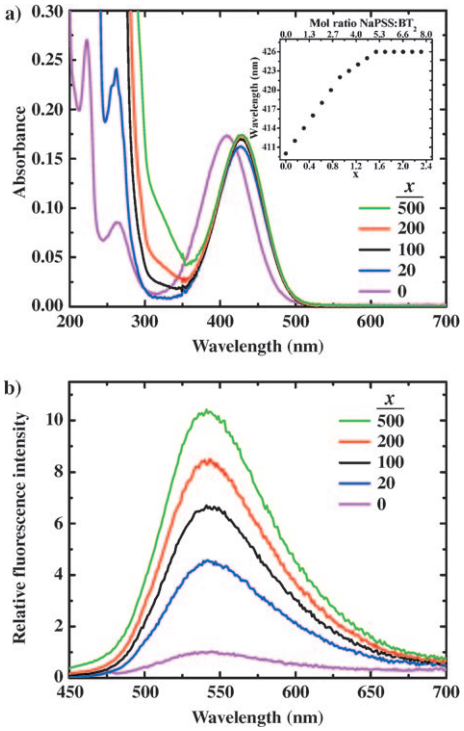

Figure 3. a) Electronic absorption and b) fluorescence emission spectra of BT_2–NaPSS (with different weight ratios NaPSS:BT_2, x) in water. The inset in (a) shows the shift of λ_{max} of the absorption at low x values. λ_{exc} for the spectra in (b) are 409 nm for pure BT_2 and 428 nm for BT_2–NaPSS.

further increase of NaPSS, the growth is less pronounced (Figure 4). As the polyelectrolyte absorption dominates in solutions with $x>500$, further studies are focused on solutions with $x=500$. Below we consider various factors that can possibly give rise to the fluorescence enhancement.

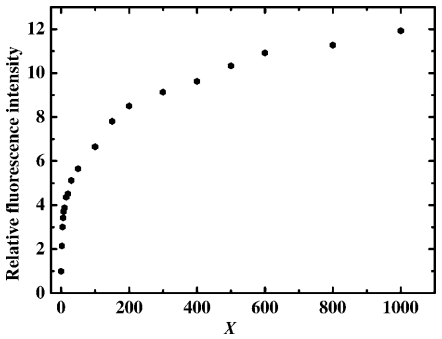

Figure 4. Variation of the intensity of fluorescence emission of BT_2 upon addition of NaPSS in aqueous solution (x = NaPSS/BT_2 weight ratio).

NaPSS has an absorption peak at 258 nm and, when excited close to this wavelength, produces a weak emission at 500 nm. Experiments on solutions of pure NaPSS, with the same molar content as in the measurements with BT_2, showed a negligible contribution to fluorescence at 542 nm at which the BT_2 emission is observed, thus ruling out a direct involvement of the polymer in the latter emission.[20] We considered another scenario wherein the absorption due to the NaPSS units at the excitation wavelength of 428 nm followed by energy transfer to the BT_2 molecules can lead to enhancement of the emission. Observation of a similar increase in the emission near 500 nm with increasing concentration of NaPSS both in the presence and absence of BT_2 rules out this possibility.[20] We also examined the possibility of increasing ionic strength of the medium affecting the fluorescence emission of BT_2, by carrying out an experiment wherein BT_2 emission in water containing increasing concentrations of sodium chloride was monitored. Even at very high salt concentrations, the enhancement of the fluorescence was found to be negligible compared with that seen in Figure 4.[20] In view of all these observations, the enhancement of fluorescence with increasing ratio of NaPSS to BT_2 appears to result from the increasing restriction of the geometry relaxation of the excited state of B^{2+}, as proposed earlier for the solid state and doped polymer films.[5]

An important question that arises at this point relates to how the polyelectrolyte restricts the geometry relaxation in B^{2+}—through local viscosity effects or molecular-level complexation mediated by ionic interactions. We carried out the following control experiments to explore the potential role of viscosity. Aqueous solutions of BT_2 mixed with the polyelectrolytes NaPSS (average molecular weight (MW)= 70000), NaPSS1 (average MW=1000000), NaCMC (sodium salt of carboxymethylcellulose, average MW= 90000), and NaPAA (sodium salt of poly(acrylic acid), average MW=170000) were prepared; the concentration of BT_2

was 10 μM and that of the polyelectrolyte 50 mM (based on monomers) in each case. The measured viscosities of the solutions are collected in Table 1. The absorption and emission spectra are shown in Figure 5. As the concentration of BT_2 is the same in all cases, the absorbances at ≈410 nm are similar. The solutions with NaPSS and NaPSS1 show slightly redshifted peaks compared to the other two samples; this is reminiscent of the observation in Figure 3a. The absence of such shifts with NaCMC and NaPAA points to the lack of strong interactions with B^{2+}. The relative fluorescence intensities estimated from the spectra are also collected in Table 1. Even though the viscosity is much higher for the mixture with NaPSS1, a consequence of the higher average molecular weight, the fluorescence is very similar to that of the mixture with NaPSS. Solutions of NaCMC and NaPAA with higher viscosities exhibit considerably lower fluorescence than that of the solution with NaPSS. These experiments suggest strongly that the bulk viscosity due to the polymer is not the determining factor for the fluorescence enhancement, but rather some molecular-level interactions. The extent of ionization of the carboxylate sites on NaCMC and NaPAA is likely to be relatively less than that of the sulfonate sites on NaPSS and NaPSS1 in the neutral aqueous solution. Therefore, any ionic complexation with B^{2+} will be more efficient in the latter two compared to the former. It is also possible that the aromatic groups in NaPSS and NaPSS1 facilitate binding with B^{2+} through favorable π interactions. We return later to an examination of the molecular-level picture of complexation between BT_2 and NaPSS.

Table 1. Viscosity and relative fluorescence intensity of aqueous solutions containing BT_2 (10 μM) and different polyelectrolytes (50 mM); see text for details of the polyelectrolytes.

Polyelectrolyte	Average molecular weight	Viscosity [cP]	Relative fluorescence intensity
NaPSS	70000	1.34–1.50	1.00
NaPSS1	1000000	6.90–7.20	1.05
NaCMC	90000	11.90–12.60	0.16
NaPAA	170000	2.90–3.30	0.10

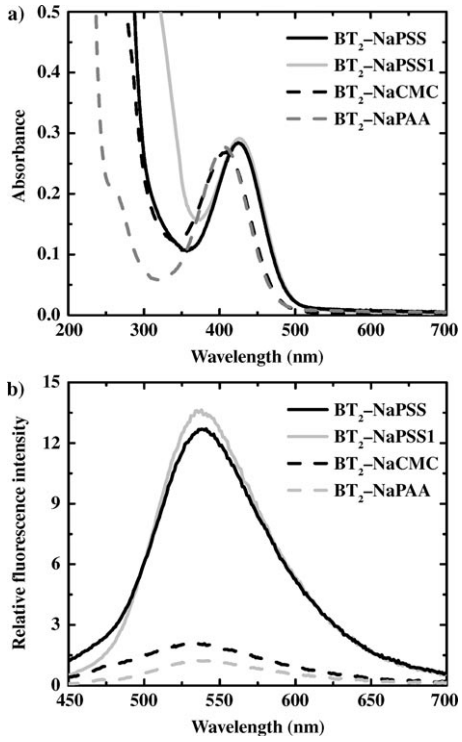

Figure 5. a) Electronic absorption and b) fluorescence emission spectra of aqueous solutions of BT_2 (10 μM) with different polyelectrolytes (50 mM); λ_{exc} for the fluorescence spectra are the λ_{max} from the corresponding absorption spectra.

In view of the preliminary insight gained from the experiments above regarding the complexation of B^{2+} with PSS^{n-} chains, and the fact that methanol is a solvent for BT_2 but not for NaPSS, we investigated the solutions/colloids obtained by injecting the aqueous solution containing BT_2 and NaPSS into methanol. Clear formation of colloids and significant spectral changes are not observed with solutions having $x<500$.[20] To assess the relevance of the water/methanol composition, we injected small aliquots (40 μL) of the aqueous solution with $x=500$ into solvent mixtures (3 mL) with increasing methanol fractions. The absorption and emission spectra of the resulting solutions/colloids are collected in Figure 6. As steep changes in the trends emerge when the fraction of methanol becomes dominant, solvent mixtures with proportions changing through closer intervals were explored in this regime (Figure 6b,d). Variation of the peak maxima and intensities of the absorption and emission with the volume fraction of methanol are plotted in Figure 7. The blueshift of the absorption when the methanol fraction increases from ≈0.3 to 0.8 possibly reflects an increasing aggregation of the ionic sites of the NaPSS chains induced by methanol and partitioning of excess water into this region, effectively increasing the dielectric constant of the local environment around B^{2+} and stabilizing its ground state. The excited state is stabilized less as its dipole moment is lower than that of the ground state, which causes the fluorescence peak also to show a blueshift; the intensity remains nearly constant in this range. The abrupt change in the absorption λ_{max} coupled with increased scattering suggest the formation of colloids when the fraction of methanol is >0.8. The fluorescence intensity shows dramatic enhancement at this point, thus indicating that the chromophores enter a rigid phase wherein the geometry relaxations are completely arrested. The most likely scenario is the formation of nano/microparticles of B^{2+} together with the styrenesulfonate units within the NaPSS aggregate structures that emerge due to the predominantly methanolic medium. Intermolecular interactions contributing to the fluorescence enhancement in these particles cannot be ruled out. Table 2 compares the relative fluorescence intensities of BT_2 and BT_2–NaPSS ($x=500$) solutions in water and the colloid formed by injecting the BT_2–NaPSS ($x=500$) aqueous solution (40 μL) into methanol (3 mL); it also lists the values of

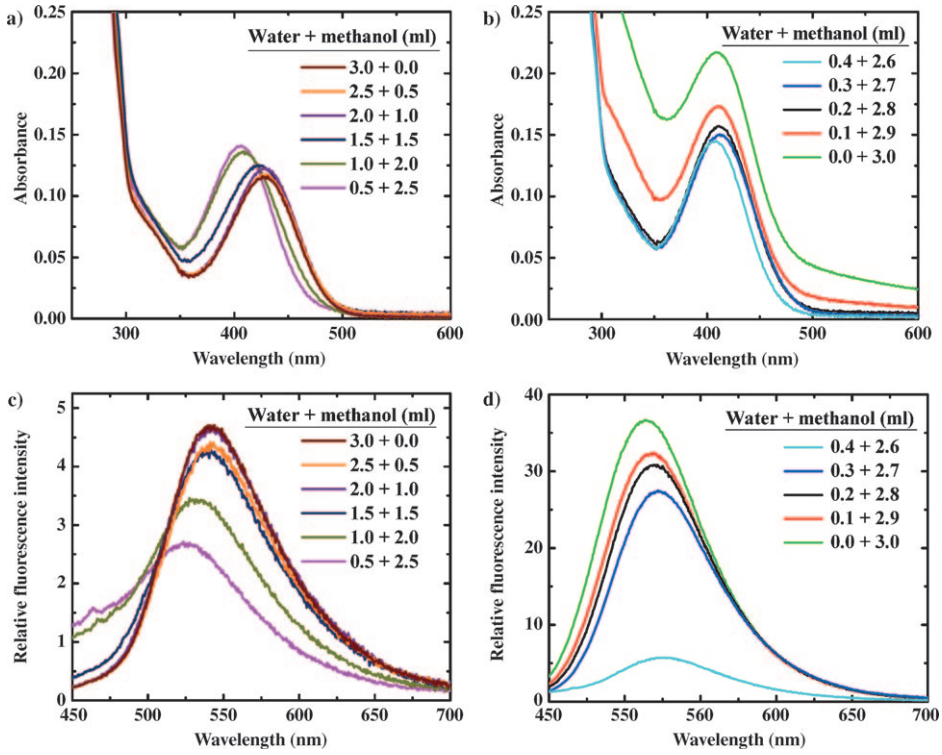

Figure 6. a,b) Electronic absorption and c,d) fluorescence emission spectra of BT_2–NaPSS ($x=500$) in water/methanol mixtures having different compositions.

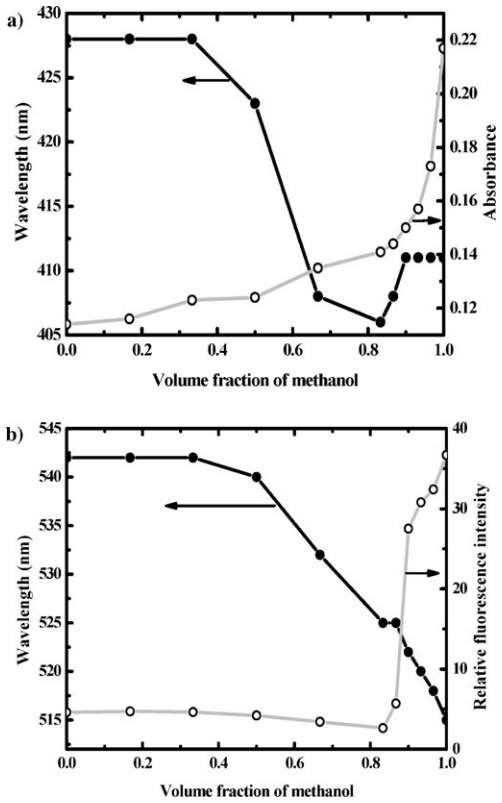

Figure 7. Variation of the λ_{max} and intensity of the a) electronic absorption and b) fluorescence emission of BT_2–NaPSS ($x=500$) in water/methanol mixtures with different fractions of methanol. The lines are only guides to the eye.

quantum yields measured in each case. The enhancement of fluorescence of the colloids formed in methanol over that of the aqueous solution of pure BT_2 is of the order of 80–100! We carried out time-resolved fluorescence measurements (with a time resolution of 40 ps) to probe the excited-state dynamics of the various systems. The fluorescence decay of BT_2 solutions in water as well as methanol was too fast to measure with the present setup. BT_2–NaPSS ($x=500$) in water decays slower and the corresponding colloid prepared in methanol even more slowly (Table 2).[20] These observations are consistent with the relative fluorescence intensities of the various systems and follow the trends expected based on the model invoking suppression of excited-state geometry relaxation leading to enhanced fluorescence.

Table 2. Relative fluorescence intensities, quantum yields, and excited-state lifetimes of BT_2 and BT_2–NaPSS solutions and BT_2–NaPSS colloid; the comparisons are based on solutions having the same molar content of BT_2.

System	Relative fluorescence intensity	Quantum yield	Lifetime[a] [ns]
BT_2 (solution in water)	1.0	0.08	<0.04
BT_2 (solution in methanol)	1.7	0.14	<0.04
BT_2–NaPSS ($x=500$; solution in water)	10.2	1.20	0.08
BT_2–NaPSS ($x=500$; colloid in methanol)	81.6	10.40	1.70

[a] Average lifetime of the excited state.

We also investigated the formation of nano/microparticles in the colloid by using different microscopy experiments. The colloids were either drop-cast on suitable substrates and dried or filtered through nanoporous membranes to prepare the samples for imaging. TEM, SEM, and AFM images are collected in Figure 8. The grainlike structures observed are ≈200–550 nm long and 100–200 nm wide. The AFM images indicate that the structures have a thickness of ≈15–25 nm. Laser confocal microscopy showed large features due to clusters of the nanoparticles; excitation of these clusters by a 458 nm laser produces emission with a peak maximum at ≈520 nm, consistent with the spectroscopic studies.[20] As BT_2 is soluble in methanol, the particles observed cannot be pure BT_2. To verify whether NaPSS forms such nanostruc-

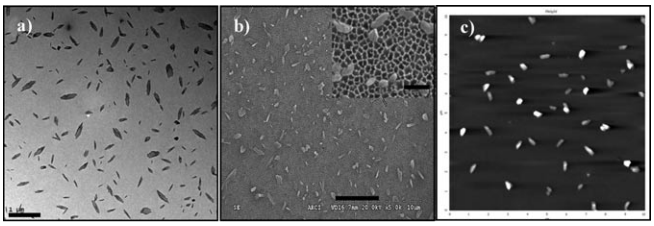

Figure 8. a) TEM (scale bar = 1 μm), b) field-emission SEM (scale bar = 5 μm; inset: scale bar = 500 nm), and c) AFM topography ($10 \times 10\ \mu m^2$) images of BT_2–NaPSS colloidal particles.

tures, aqueous solutions of NaPSS were injected into methanol (keeping the concentrations and volumes of solutions the same as in the case of BT_2–NaPSS) and the resulting colloids examined. Only some diffuse aggregates were obtained and no structures similar to those in Figure 8 could be found.[20] These experiments prove that the particles are indeed formed by the aggregation of BT_2 with NaPSS. The fine details of whether crystals of BT_2 are formed embedded inside the polyelectrolyte chains or the two are enmeshed in an aggregate structure are not clear at the moment.

To gain insight into the nature of the molecular interactions between B^{2+} and PSS^{n-}, we carried out ITC experiments by titrating aqueous solutions of NaPSS into aqueous solutions of BT_2. In a typical experiment, a 0.05 mM solution of BT_2 (1.44 mL) was placed in the cell and aliquots (7 μL) of a 2 mM solution of NaPSS were injected at time intervals of 240 s (first injection alone was 2 μL). The thermograms (raw and integrated) obtained are shown in Figure 9. The heat changes follow a complicated pattern and the full thermogram cannot be fitted to standard binding models. However, some salient features of the molecular interaction can be inferred. Appreciable heat changes that remain nearly constant up to a molar ratio of ≈2.0 are indicative of a strong binding interaction. In the molar ratio range 2.0–4.0, the heat changes diminish and tend towards zero. This points to a binding stoichiometry in this range, that is, about three monomer sites per B^{2+} unit. As PSS^{n-} is almost completely sulfonated,[20] this implies that one B^{2+} ion engages two sulfonate sites, and on average an additional one becomes unavailable for binding further B^{2+} possibly due to steric congestion. If the binding events were completed following this process, the thermogram would have approached zero heat change smoothly. However, a further small dip appears near the molar ratio of ≈5.0, which indicates possible aggregation of the polyelectrolyte chains. As these special features of the thermogram are quite reproducible, we attempted a partial fitting of the data in the low molar ratio regime (0.4–4.0) to a single-site binding model; it may be noted that such partial analysis is common with systems showing complex behavior.[21] The fitting is shown in Figure 9b; the parameters estimated (Table 3) are consistent with the general inferences drawn above.

To confirm the significance of these observations, we carried out a control experiment with an analogue of BT_2, 7,7-bis(*N*-methylpiperazino)-8,8-dicyanoquinodimethane (BMPDQ).[5] BMPDQ has exactly the same fluorophore unit as B^{2+}, but has no net charge as *N*-methyl replaces ammonium as the remote group. The thermogram recorded for the titration against NaPSS is very different;[20] even though some binding interaction is observed (possibly due to the highly dipolar structure of BMPDQ, similar to that of B^{2+}), it is considerably weaker (the difference appears to be primarily entropy driven) and the stoichiometry is ≈0.7 (Table 3). No binding interaction is observed at higher stoichiometries. Parallel spectroscopic experiments indicate fluorescence enhancement in aqueous solutions of BMPDQ–NaPSS; however, when injected into methanol medium, the enhancement is significantly lower than that

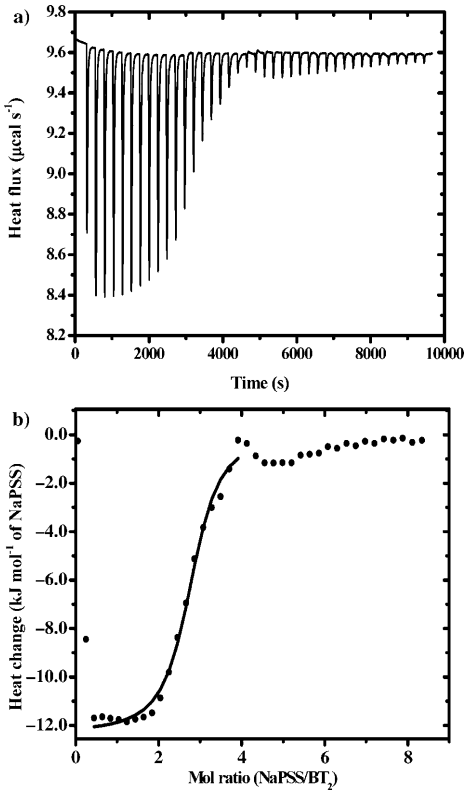

Figure 9. a) Raw and b) integrated thermograms from the isothermal titration of NaPSS (2 mM) into BT_2 (0.05 mM) in aqueous solution. Partial fitting of the integrated thermogram is also shown.

Table 3. Binding and thermodynamic parameters from the ITC experiments on NaPSS against BT_2 and BMPDQ. The percentage error for the parameters estimated by the nonlinear least-squares fitting are indicated in brackets; the fitting was carried out for molar ratios in the range 0.4–4.0 in both cases.

Parameter	Value [% error]	
	BT_2–NaPSS	BMPDQ–NaPSS
N (stoichiometry)	2.73 [1.1]	0.67 [1.2]
K [$dm^3\,mol^{-1}$]	4.4×10^5 [15.3]	1.0×10^4 [18.6]
$\Delta H°$ [$kJ\,mol^{-1}$]	−12.3 [1.5]	−12.8 [13.9]
$\Delta G°$ [$kJ\,mol^{-1}$]	−32.2	−22.9
$\Delta S°$ [$J\,mol^{-1}\,K^{-1}$]	66.5	33.9

observed in BT_2–NaPSS.[20] All these facts indicate that B^{2+} has a unique and strong binding interaction with the PSS^{n-}, and this complexation is followed by further aggregation of the polyelectrolyte chains and colloidal particle formation when injected into methanol.

Taking into account the various spectroscopic and calorimetric investigations and the microscopy observation of the nano/microparticles, a model can be developed for the molecular systems existing in the various environments and their optical responses. Figure 10 shows schematically the complexation of B^{2+} with PSS^{n-} in water and the enhancement of fluorescence as a consequence of the partial rigidification. Upon further addition of NaPSS, the fluorescence increases further, as a result of the aggregation of the polyelectrolyte chains around the complex. Injection into methanol/water mixtures with an increasing fraction of methanol causes these aggregates to tighten due to the insolubility of NaPSS in methanol, and collect water preferentially into their fold. When the medium is almost completely methanol (except for the trace quantity of water in the injectant), the aggregation of BT_2–NaPSS or the B^{2+}–PSS^{n-} complex into particles is complete and the total rigidification of B^{2+} leads to the final enhancement of the fluorescence response. Control experiments carried out with a simple sulfonate surfactant, sodium dodecylbenzenesulfonate, in place of NaPSS showed that even though complexation occurs in aqueous medium, as revealed by absorption spectral shifts, the colloid formed in methanol is not stable and exhibits no fluorescence enhancement.[20] This demonstrates clearly the critical role played by the polyelectrolyte chains in the formation of the colloids and fluorescence enhancement as described above.

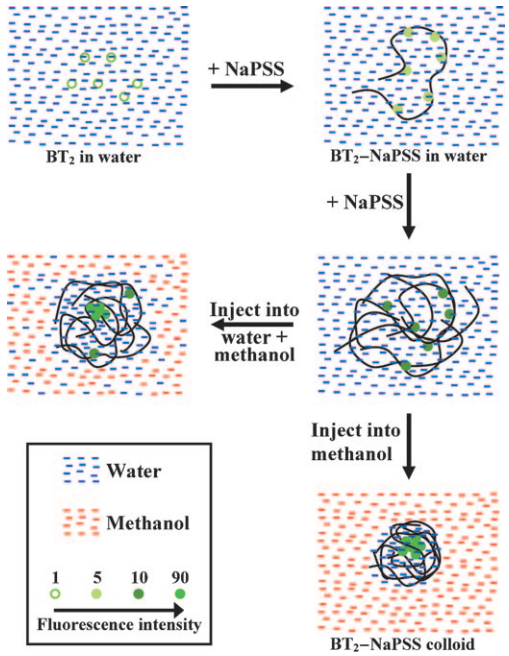

Figure 10. Schematic representation of the model proposed to explain the observed fluorescence enhancement in BT_2–NaPSS systems; the symbols used in the representation are explained in the legend box.

Conclusion

We have demonstrated a polyelectrolyte-assisted reprecipitation protocol for the fabrication of highly fluorescent colloidal nanoparticles of a zwitterionic diaminodicyanoquinodimethane molecule, BT_2. This family of molecules is known to show enhanced fluorescence in the aggregated and solid states but, due to high solubility, these compounds are not amenable to the simple reprecipitation method commonly used to prepare molecular nano/microcrystals. Electrostatic binding of B^{2+} with the polyanion and the aggregation of the polyelectrolyte chains in water lead to partial rigidification of the fluorophore and enhanced emission. Transfer to methanol induces colloid formation due to the insolubility of the polyelectrolyte and aggregation of the B^{2+}, with significant enhancement of the emission intensity. Spectroscopy, microscopy, and calorimetry investigations including several control experiments are used to formulate a model that helps to visualize the fundamentally interesting dye–polyelectrolyte interaction, and explain the observed emission enhancement. This method should prove generally useful for the preparation of molecular nanocrystals capable of aggregation-induced emission. An important extension of these studies that warrants detailed exploration is the aggregation of fluorophores and enhancement of emission in thin polymer films formed by various methods including layer-by-layer assembly.

Experimental Section

Synthesis and colloid fabrication: BT_2 was prepared by following the reported procedure with minor modifications, recrystallized thrice from high-purity water (Millipore Milli-Q, resistivity = 18 MΩ cm), and characterized.[5,17,20] NaPSS (Aldrich, average MW = 70000) was purified by dissolution in high-purity water followed by precipitation with methanol, centrifugation, filtration, and drying under vacuum. The purity and extent of sulfonation (>95%) were confirmed by NMR spectroscopy.[20,22] Solutions of BT_2–NaPSS and their nano/microparticles were prepared as follows. Solutions of BT_2 (1 mM) and NaPSS (1 M) in high-purity water were mixed to prepare BT_2–NaPSS mixtures with a wide range of weight ratios; the pH of all solutions at 25 °C was found to be ≈6.0. Colloids were prepared by injecting the solution (x = 500; 40 μL) rapidly into methanol (3 mL) at 25 °C under ultrasonication which was continued for 2 min.

Absorption and fluorescence spectroscopy: Electronic absorption spectra were recorded on a Varian Cary 100 UV/Vis spectrometer. Steady-state fluorescence emission and excitation spectra were recorded on a Horiba Jobin Yvon Model FL3-22 Fluorolog spectrofluorimeter. The optical density of the solution and colloid samples was maintained at <0.3 by appropriate dilution to avoid inner-filter effects. The fluorescence quantum yield was determined by comparison with quinine sulfate solution in 1 N H_2SO_4 (Φ_f = 0.546).[23] Absolute measurements of quantum yield were also carried out, by using the integrating sphere and the software supplied by the spectrofluorimeter manufacturer. Time-resolved fluorescence measurements were carried out with a time-correlated single-photon-counting spectrometer (IBH NanoLED). A diode laser (λ_{exc} =

405 nm, full width at half maximum = 95 ps) was used as the excitation source and a microchannel-plate photomultiplier (Hamamatsu R3809U-50) as the detector. The lamp profile was recorded by placing a scatterer (dilute solution of Ludox in water) in place of the sample. Decay curves were analyzed by nonlinear least-squares iteration with IBH DAS6 (Version 2.2) decay analysis software.

Viscosity measurements: Viscosity measurements were carried out at 25 °C by using a Brookfield Viscometers model LVDV-IIIUCP rheometer. Measurements were carried out on solutions prepared by adding an aqueous solution of BT_2 (50 μL, 1 mM) to aqueous solutions (5 mL, 50 mM) of each of the polymers: NaPSS (Aldrich, average MW = 70000), NaPSS1 (Aldrich, average MW = 1000000), NaCMC (Aldrich, average MW = 90000), and NaPAA (Aldrich, average MW = 170000).

Microscopy: The size and morphology of the colloidal nano/microparticles were examined by using i) an FEI model TECNAI G^2 20 S-Twin TEM instrument, ii) Philips Model XL30 SEM and Hitachi model S-4300SE/N FESEM instruments, iii) an NT-MDT Model Solver Pro M AFM instrument, and iv) a Leica model TCS SP2 AOBS laser scanning confocal microscope. The samples for TEM were prepared by placing a drop of the colloidal solution on a copper grid and drying under ambient conditions; the accelerating voltage used was 120 kV. The colloidal solution was dip-coated on a clean glass substrate, dried in air, and used in the AFM investigations; imaging was carried out in the semicontact mode by using a cantilever with a force constant of 10 $N m^{-1}$. Samples for the FESEM and SEM studies were prepared by filtering the colloidal solution through a 100 nm pore aluminum oxide membrane (Anodisc, Whatman) and coating with a thin layer of sputtered gold; a 20 kV beam voltage was used. Samples for confocal microscopy were prepared by drop-casting on a clean glass substrate; $\lambda_{exc} = 458$ nm, $\lambda_{em} = 475$–580 nm.

ITC: A Microcal Model VP-ITC isothermal titration calorimeter was used to carry out the calorimetric experiments to probe the complexation of BT_2 (and BMPDQ) with NaPSS in aqueous solution. All studies were carried out at 298 K. Unlike the normal practice of titrating ligand into the protein (polymer) solution, the solution of NaPSS was titrated into BT_2 as a parallel to our spectroscopic studies. Water was used in the reference cell. A control experiment, in which NaPSS was injected into pure water in the cell, was used to correct the measured heats for dilution effects. Origin 7.0-based software provided by the manufacturer was used to analyze the data.

Acknowledgements

Financial support from the Department of Science and Technology, New Delhi, and infrastructure support from the Centre for Nanotechnology and the Central Instrumentation Laboratory at the University of Hyderabad are acknowledged with gratitude. We thank Prof. M. J. Swamy and A. Narahari for help with the ITC experiments, Prof. A. Samanta and K. Santhosh for help with the fluorescence decay studies, and Prof. M. Durga Prasad for fruitful discussions. C.G.C. thanks CSIR, New Delhi, for a senior research fellowship.

[1] a) J. Luo, Z. Xie, J. W. Y. Lam, L. Cheng, H. Chen, C. Qiu, H. S. Kwok, X. Zhan, Y. Liu, D. Zhu, B. Z. Tang, *Chem. Commun.* **2001**, 1740; b) Y. Hong, J. W. Y. Lam, B. Z. Tang, *Chem. Commun.* **2009**, 4332.

[2] a) R. Deans, J. Kim, M. R. Machacek, T. M. Swager, *J. Am. Chem. Soc.* **2000**, *122*, 8565; b) M. Levitus, K. Schmieder, H. Ricks, K. D. Shimizu, U. H. F. Bunz, M. A. Garcia-Garibay, *J. Am. Chem. Soc.* **2001**, *123*, 4259.

[3] a) B. K. An, S. K. Kwon, S. D. Jung, S. Y. Park, *J. Am. Chem. Soc.* **2002**, *124*, 14410; b) T. Hirose, K. Matsuda, *Chem. Commun.* **2009**, 5832.

[4] J. N. Wilson, M. D. Smith, V. Enkelmann, U. H. F. Bunz, *Chem. Commun.* **2004**, 1700.

[5] S. Jayanty, T. P. Radhakrishnan, *Chem. Eur. J.* **2004**, *10*, 791.

[6] a) D. Bloor, Y. Kagawa, M. Szablewski, M. Ravi, S. J. Clark, G. H. Cross, L. Pålsson, A. Beeby, C. Parmer, G. Rumbles, *J. Mater. Chem.* **2001**, *11*, 3053; b) M. Szablewski, D. Bloor, Y. Kagawa, R. Mosurkal, J. M. Cole, S. J. Clark, G. H. Cross, L. Pålsson, *J. Phys. Org. Chem.* **2006**, *19*, 206.

[7] R. Davis, N. S. S. Kumar, S. Abraham, C. H. Suresh, N. P. Rath, N. Tamaoki, S. Das, *J. Phys. Chem. C* **2008**, *112*, 2137.

[8] a) Y. Dong, J. W. Y. Lam, A. Qin, J. Sun, J. Liu, Z. Li, S. Zhang, J. Sun, H. S. Kwok, B. Z. Tang, *Appl. Phys. Lett.* **2007**, *91*, 011111; b) Z. Zhao, S. Chen, X. Shen, F. Mahtab, Y. Yu, P. Lu, J. W. Y. Lam, H. S. Kwok, B. Z. Tang, *Chem. Commun.* **2010**, *46*, 686.

[9] a) H. Oikawa, H. Kasai, H. Nakanishi, *ACS Symp. Ser.* **2001**, *798*, 158; b) Y. S. Zhao, H. Fu, A. Peng, Y. Ma, D. Xiao, J. Yao, *Adv. Mater.* **2008**, *20*, 2859; c) Q. Fang, F. Wang, H. Zhao, X. Liu, R. Tu, D. Wang, Z. Zhang, *J. Phys. Chem. B* **2008**, *112*, 2837.

[10] a) E. I. Mal'tsev, D. A. Lypenko, B. I. Shapiro, M. A. Brusentseva, V. I. Berendyaev, B. V. Kotov, A. V. Vannikov, *Appl. Phys. Lett.* **1998**, *73*, 3641; b) L. Jinshui, W. Lun, G. Feng, L. Yongxing, W. Yun, *Anal. Bioanal. Chem.* **2003**, *377*, 346; c) E. Botzung-Appert, V. Monnier, T. Ha Duong, R. Pansu, A. Ibanez, *Chem. Mater.* **2004**, *16*, 1609; d) L. Wang, L. Wang, L. Dong, G. Bian, T. Xia, H. Chen, *Spectrochim. Acta Part A* **2005**, *61*, 129.

[11] a) A. Patra, N. Hebalkar, B. Sreedhar, M. Sarkar, A. Samanta, T. P. Radhakrishnan, *Small* **2006**, *2*, 650; b) A. Patra, N. Hebalkar, B. Sreedhar, T. P. Radhakrishnan, *J. Phys. Chem. C* **2007**, *111*, 16184.

[12] A. Patra, N. Venkatram, D. N. Rao, T. P. Radhakrishnan, *J. Phys. Chem. C* **2008**, *112*, 16269.

[13] A. Patra, S. P. Anthony, T. P. Radhakrishnan, *Adv. Funct. Mater.* **2007**, *17*, 2077.

[14] H. Nakanishi, H. Oikawa in *Single Organic Nanoparticles* (Eds.: H. Masuhara, H. Nakanishi, K. Sasaki), Springer, Berlin, **2003**, pp. 17–31.

[15] a) F. Bertorelle, D. Lavabre, S. Fery-Forgues, *J. Am. Chem. Soc.* **2003**, *125*, 6244; b) H. Fu, D. Xiao, J. Yao, G. Yang, *Angew. Chem.* **2003**, *115*, 2989; *Angew. Chem. Int. Ed.* **2003**, *42*, 2883; c) X. Zhang, X. Zhang, W. Shi, X. Meng, C. Lee, S. Lee, *J. Phys. Chem. B* **2005**, *109*, 18777; d) M. Abyan, D. de Caro, S. Fery-Forgues, *Langmuir* **2009**, *25*, 1651.

[16] a) S. Abe, L. Chen, *J. Polym. Sci. Polym. Chem. Ed* **2003**, *41*, 1676; b) A. Diaspro, S. Krol, B. Campanini, F. Cannone, G. Chirico, *Opt. Express* **2006**, *14*, 9815; c) S. Meyer, P. Pescador, E. Donath, *J. Phys. Chem. C* **2008**, *112*, 1427.

[17] S. Jayanty, T. P. Radhakrishnan, *Chem. Mater.* **2001**, *13*, 2460.

[18] C. Peyratout, E. Donath, L. Daehne, *J. Photochem. Photobiol. A* **2001**, *142*, 51.

[19] a) M. Ravi, T. P. Radhakrishnan, *J. Phy. Chem.* **1995**, *99*, 17624; b) J. M. Cole, R. C. B. Copley, G. J. McIntyre, J. A. K. Howard, M. Szablewski, G. H. Cross, *Phys. Rev. B* **2002**, *65*, 125107.

[20] See the Supporting Information.

[21] a) S. Hakkarainen, S. L. Gilbert, A. Kontturi, K. Kontturi, *J. Colloid Interface Sci.* **2004**, *272*, 404; b) Y. Lapitsky, M. Parikh, E. W. Kaler, *J. Phys. Chem. B* **2007**, *111*, 8379.

[22] D. Baigl, T. A. P. Seery, C. E. Williams, *Macromolecules* **2002**, *35*, 2318.

[23] J. N. Demas, G. A. Crosby, *J. Phys. Chem.* **1971**, *75*, 991.

Received: February 25, 2010
Published online: June 23, 2010

